fundamental steps involved in fertilization, gene programming and expression, regulation of the cell cycle and patterns of differentiation.

The first babies born after transfer of embryos that had been frozen and thawed were born in 1984-85, and cryopreservation of embryos as well as semen became routine. Experiments with cell cultures and co-culture allowed the development of stage-specific media optimized for embryo culture to the blastocyst stage. Advances in techniques and micromanipulation technology led to the establishment of assisted fertilization (intracytoplasmic sperm injection) by a Belgian team led by André Van Steirteghem and including Gianpiero Palermo (Palermo et al. 1992) by the mid 1990s. Other microsurgical interventions were then introduced, such as assisted hatching and embryo biopsy for genetic diagnosis. Gonadal tissue cryopreservation, *in vitro* oocyte maturation and embryonic stem cell culture are now under development as therapeutic instruments and remedies for the future.

Applications in Veterinary Science

The first live calves resulting from bovine IVF were born in the USA in 1981. This further milestone in reproductive biotechnology inspired the development of IVF as the next potential commercial application of assisted reproduction in domestic species, following on from artificial insemination and conventional transfer of embryos produced *in vivo* from superovulated donors. The assisted reproductive techniques continued to be refined so that by the 1990s IVF was integrated into routine domestic species breeding programmes. Equine IVF has also been introduced into the world of horse breeding (although reproductive technology procedures cannot be used for thoroughbreds). China used artificial insemination to produce the first giant panda cub in captivity in 1963, and assisted reproduction is now used in the rescue and propagation of endangered species, from pandas and large cats to dolphins. Artificial insemination, and, in some cases, IVF are used routinely in specialist zoos throughout the world.

Somatic cell nuclear transfer into enucleated oocytes has created 'cloned' animals in several species, the most famous being Dolly the sheep, who was born in Edinburgh in 1997 and was euthanized at an early age in February 2003, after developing arthritis and progressive lung disease.

Advances in molecular biology and biotechnology continue to be applied in assisted reproductive technology. Preimplantation genetic diagnosis, introduced in 1988, is used to screen embryos for sex-linked diseases or autosomal mutations in order to exclude chromosomally abnormal embryos from transfer. Molecular biology techniques can identify chromosomes with the use of fluorescently labelled probes for hybridization, or amplify DNA from a single blastomere using the polymerase chain reaction. This technique is also used for gender selection, now used routinely in animal breeding programmes.

Authors have confirmed where relevant, that experiments on animals and man were conducted in accordance with national and/or local ethical requirements.

C1

Transient and sustained synaptic activity in the retina of zebrafish imaged using a genetically encoded calcium indicator

E. Dreosti, B. Odermatt and L. Lagnado

Neurobiology, MRC Laboratory of Molecular Biology, Cambridge, UK

Retinal bipolar cells play a key role in the processing of the visual signal because they are the only neurons transmitting information directly from photoreceptors providing the input to ganglion cells, which deliver the output. The ON class of bipolar cells are depolarized by an increase in light intensity, while OFF cells are hyperpolarized. Bipolar cells also contribute to the temporal filtering of the visual input into sustained and transient channels responding preferentially to slow or fast changes in light intensity (Masland, 2001). It is still unclear how the ribbon-type synapses of bipolar cells transmit voltage signals of opposite polarities and different kinetics.

To monitor synaptic activity of bipolar cells, operating within the intact retinal circuit, we have made transgenic zebrafish expressing a new genetically-encoded reporter of synaptic activity. This reporter, SyGCaMP2, is composed of the calcium-sensitive fluorescent construct GCaMP2 (Tallini, 2006) fused to the synaptic vesicle protein synaptophysin. SyGCaMP2 was put under control of a promoter driving expression in ribbon synapses and calcium signals monitored across tens to hundreds of terminals in the inner retina by multiphoton microscopy. Zebrafish 9-12 days post-fertilization were anaesthetised by immersion in 0.016% MS222, immobilized in low melting agarose and injected with α-bungarotoxin (2mg/ml). Both spontaneous and light-driven activity were monitored through all the strata of the inner plexiform layer at rates up to 200 Hz and across one stratum at 1 kHz.

We observed two basic types of presynaptic calcium signal in response to light: slow, sustained changes and faster calcium "spikes". Sustained increases or decreases in calcium were observed in ON or OFF cells respectively, and were maintained throughout exposure to a step of light. These slow calcium signals are expected to modulate the rate at which vesicles are cycled through rounds of exocytosis and endocytosis (Lagnado et al., 1996). Calcium "spikes" were observed in both ON and OFF cells, rising to a peak in about 50 ms and declining in seconds. These fast signals are likely to reflect regenerative electrical activity through L-type calcium channels in the synaptic terminal (Burrone and Lagnado, 1997), which will trigger fast, transient, modes of exocytosis (Burrone, 2000). Individual bipolar cells transmitting in different strata of the IPL did not necessarily generate presynaptic calcium signals with the same kinetics: sustained signals were observed in some terminals and transient signals in others. These observations suggest that the basic unit for the generation of transient signals from the bipolar cells is the synaptic terminal rather than the whole neuron.

Masland RH (2001). Nat Neurosci 4, 877-886.

Tallini YN et al. (2006). Proc Natl Acad Sci USA 103, 4753-4758.

Lagnado L et al. (1996). Neuron 17, 957-967.

Burrone J & Lagnado L (1997). J Physiol 15, 571-584.

Burrone J et al. (2000) J Neurosci 20, 568-578.

Funded by the MRC LMB, the European Cambridge Trust and the Wellcome Trust.

Authors have confirmed where relevant, that experiments on animals and man were conducted in accordance with national and/or local ethical requirements.

C2

Activity-dependent, input-specific depression of neuron-glial transmission in the cerebellum

S. Balakrishnan and T.C. Bellamy

Molecular Signalling, Babraham Institute, Cambridge, UK

The cerebellar Purkinje cell receives two inputs: a single climbing fibre (CF) and many thousands of parallel fibres (PF). These synapses are each surrounded by a glial sheath, formed from the processes of specialized astrocytes, the Bergmann glial cells. Bergmann glia express Ca^{2+}-permeable AMPA receptors and electrogenic glutamate transporters, which evoke inward currents following PF or CF stimulation, providing a pathway for neuron-glial transmission. We previously reported, using whole cell patch clamp recordings in juvenile (16-20 day) rat cerebellar slices, that repetitive stimulation of PFs in the 0.1-1 Hz range depresses this neuron-glial transmission without overt effect on the strength of transmission at adjacent synapses (Bellamy and Ogden, 2006), demonstrating that these ancillary pathways can express plasticity independently of the synaptic network. We have now investigated the specificity of this neuron-glial plasticity.

Stimulation of CFs in the 0.1-1 Hz range led to depression of glial currents, in a closely similar manner to that observed at PFs. Depression of the two inputs was independent: either PF or CF inputs could be depressed by raising stimulation frequency from 0.033 to 1 Hz, without affecting the strength of the other input. Furthermore, by stimulation of proximal and distal regions of the molecular layer, we found that separate PFs could be independently depressed, indicating that the decrease in AMPAR and transporter current amplitude was not due to a general desensitization of the glial cell or a change in cable properties. Finally, stimulation of granule neurons in the granular layer rather than molecular layer, so as to activate PF synapses over a distributed area of the Purkinje and Bergmann glial cells, also exhibited depression of glial currents (enhanced by preincubation with 50 μM cyclothiazide), indicating that crosstalk between adjacent PF is not necessary for neuron-glial plasticity.

These findings demonstrate specific and dynamic regulation of the strength of neuron to glial signalling at the major synapses in the cerebellum.

Bellamy T.C. and Ogden D. (2006) Eur. J. Neurosci. 23, 581-586.

Authors have confirmed where relevant, that experiments on animals and man were conducted in accordance with national and/or local ethical requirements.

C3

A Ca^{2+}-ATPase-mediated alkalinization on the surface of individual CA1 neurons in mouse hippocampal slices

S. Makani and M. Chesler

Neuroscience and Physiology, New York University, New York, NY, USA

Synchronous neural activity causes an extracellular alkaline transient (AT) in a variety of preparations [1]. This pH change is especially robust in hippocampus, and has been shown to boost synaptic NMDA receptor responses [2]. The main hypothesis for the mechanism underlying the AT is that depolarization-induced Ca^{2+} influx activates the plasma membrane Ca^{2+}-ATPase (PMCA), which exchanges intracellular Ca^{2+} for extracellular H^+ [3]. Activation of the PMCA should increase surface pH, as has been demonstrated on snail neurons [3] and retinal cells of the catfish [4]. We sought to determine: (a) if such a rise in surface pH could be detected on neurons in mouse hippocampal slices, and (b) if this surface AT could explain the large extracellular ATs evoked by synchronous activity. This was made feasible by the use of high-speed, low-noise, concentric pH microelectrodes [5] placed against the surface of single CA1 pyramidal neurons, voltage clamped (to -60 mV) by a second pipette. The carbonic anhydrase inhibitor benzolamide (BZ; 10 μM) was included in the saline to maximize surface ATs. Using 20 mV steps, hyperpolarizing the cell to –120 mV did not affect surface pH. Depolarizing the cell to +40 mV caused a rapid AT, which peaked at 0 mV (0.02 ± 0.002 unit pH (mean ± SEM); n=5). The changes recorded with the pH electrode were never seen when it was replaced by a 2M NaCl-filled micropipette, and were markedly reduced by adding a small amount of HEPES buffer, indicating that the electrode responses represented pH changes. Addition of 1, 5, or 20 mM HEPES reduced the AT by 43 ± 7.3, 91 ± 5.7, and 98 ± 1.6%, respectively (n=5 and $p<0.01$ (paired t-test) for all). In experiments where BZ was not added to control saline, a small surface AT was evoked (0.01 ± 0.002 unit pH, n=5), and was increased by 356 ± 100% ($p<0.02$) after addition of BZ. Addition of Cd2+ (300 μM) reduced the surface AT by 71 ± 14% (n=6; $p<0.002$). Bath addition of the PMCA inhibitor 5(6)-carboxyeosin (CE; 200 μM) reduced the surface AT by 65 ± 14% ($p<0.05$). Addition of CE (0.5 μM) to the patch pipette reduced the AT by 88 ± 7.5% five min. after breakthrough to whole cell mode (n=5; $p<0.05$), whereas the response remained stable for more than 5 min. without intracellular CE (n=5; $p=0.28$). To simulate the response to repetitive antidromic stimulation, a 2 sec 100 Hz spike train was used as the voltage clamp command. This elicited a similar surface AT that was inhibited 71 ± 19% by bath addition of CE. By contrast, real antidromic stimulation of the CA1 pyramidal neuron population elicited an extracellular AT that was not inhibited by bath-applied CE (n=7 slices). These results indicate that while activation of single pyramidal neurons evokes the anticipated CE-sensitive rise in surface pH, the AT elicited by synchronous activity cannot be similarly attributed to the neuronal PMCA.

Chesler M (2003). Physiol Rev 83, 1183-1221.

Makani S & Chesler M (2007). J Neurosci 27: 7438-7446.

Schwiening CJ et al (1993). Proc R Soc Lond B Biol Sci 253: 285-289.

Kreitzer et al (2007). J Gen Physiol 130: 169-182.

Fedirko N et al (2006). J Neurophysiol 96: 919–924.

Authors have confirmed where relevant, that experiments on animals and man were conducted in accordance with national and/or local ethical requirements.

C4

Human cortical neurones in tissues from epilepsy surgery have a reduced chloride extrusion

R.A. Deisz[1], T.N. Lehmann[2], C. Dehnicke[3] and R. Nitsch[1]

[1]Cell- and Neurobiology, Charite, Berlin, Germany, [2]Neurosurgery, Charite, Berlin, Germany and [3]Epilepsiecenter, KEH, Berlin, Germany

In cortical neurones, E_{GABA} is governed by a low intracellular chloride, maintained by a K^+-coupled outward transport for Cl^- (Thompson et al. 1988), and the bicarbonate gradient (Kaila et al. 1993). Neurones in slices from human epileptogenic tissues, however, exhibit a depolarising $GABA_A$ inhibition (Deisz et al., 1998, Cohen et al. 2002). We further evaluated these depolarising $GABA_A$ responses and the underlying mechanisms. Layer 2/3 neurons were investigated in slices of human cortical tissues from epilepsy surgery with sharp microelectrode recordings (for methods see Deisz, 1999). Kinetics of anion transport mechanisms, were evaluated by monitoring the $IPSP_A$ amplitudes before, during and after injections of anions. $IPSP_A$ were pharmacologically isolated by ACSF containing 10μM CNQX, 20μM D-APV and 2μM CGP55845A (CDC-ACSF). With K-acetate filled electrodes, the reversal potentials of the composite EPSP and IPSP response of human neurones averaged -54.2±10.6mV (mean±s.d.; E_m:-71.5±4.8 mV, n=82) in control condition and –61.5±8.5mV (E_m:-71.4±6.5mV, n=46) in CDC-ACSF. Of these 46 neurones, 20 had an E_{IPSP} more negative than –65mV, on average -69.5±2.7mV, whereas the E_{IPSP} of the other 26 averaged –56.5±5.7mV (P<0.001, t- test). After current injection from KCl-filled electrodes, the $IPSP_A$ recovered with a time constant (τ) of 18.3±5.9s in CDC-ACSF (n=17), close to control values (21.5±8.4s, n=24; P=0.24) in ACSF. Only two neurones exhibited a τ below 10s. Bath application of furosemide (200μM) in CDC-ACSF reversibly increased the amplitudes of $IPSP_A$ (from 7.9 ±5.1mV to 11.6±7.9 mV, n=5, P=0.034) and increased τ of recovery from 16.3±7.5s to 44.3±9.5s (n=5, P=0.002). Application of bumetanide (50μM) had no effect on the amplitudes of isolated $IPSP_A$ (control: 6.3±4.5mV, bumetanide: 6.6±4.9mV; n=6, P>0.5) and increased the τ of recovery from 19.4±4.4s to 25.7±1.5s (n=5; P=0.017). The τ after injection of nitrate (not carried by KCC2) averaged 34.9±11.2s (n=4. Preliminary experiments using reduction of K^+_o from 5 to 2.5mM had no effect on τ of recovery. To validate our methods, we evaluated the kinetics of Cl^- extrusion also in rat cortical neurones. The t from Cl^- injection averaged 8.7±3.0s (n=17) in CDC-ACSF. Bumetanide and furosemide increased τ from 6.9±1.2s to 9.3±2.4s (n=7; P=0.036) and from 6.6±1.3s to 14.1±1.3s (n=3), respectively. Preliminary data from rat neurones indicate that reduction of K^+_o decreased τ of recovery from about 10s to 7s. The data indicate an impaired Cl^- extrusion in some human cortical neurones from epileptogenic tissues. The reduced Cl^- extrusion may contribute to elevated Cl^-_i, particularly by synaptic Cl^- fluxes. It remains to be determined whether impairments of Cl^- homeostasis relate to the severity of epilepsy.

Deisz, R.A., Lehmann, T.N., Lanksch, W.R., Meencke, H.J. & Nitsch, R. (1998). Receptor mechanisms involved in hyperexcitability of cortical tissue from epilepsy surgery. Journal of Physiology 513, 35-36P.

Deisz, R.A. (1999). GABAB receptor-mediated effects in human and rat neocortical neurones in vitro. Neuropharmacology 38, 1755-1766.

Cohen, I., Navarro, V., Clemenceau, S., Baulac, M. & Miles, R. (2002). On the origin of interictal activity in human temporal lobe epilepsy in vitro. Science 298,1418-1421.

Kaila, K., Voipio, J., Paalasmaa, P., Pasternack, M. & Deisz, R.A. (1993). The role of bicarbonate in GABAA receptor-mediated IPSPs of rat neocortical neurones. Journal of Physiology 464, 273-289.

Thompson, S.M., Deisz, R.A. & Prince, D.A. (1988). Relative contributions of passive equilibrium and active transport to the distribution of chloride in mammalian cortical neurons. Journal of Neurophysiology 60, 105-124.

We gratefully acknowledge financial support from the Sonnenfeld foundation.

Authors have confirmed where relevant, that experiments on animals and man were conducted in accordance with national and/or local ethical requirements.

C5

Volume diffusion of nitric oxide at a glutamatergic synapse in mouse auditory brainstem

J.R. Steinert[1], C. Baker[1], J. Challiss[2], R. Mistry[2], B.P. Graham[3] and I.D. Forsythe[1]

[1]MRC Toxicology Unit, Leicester, UK, [2]Department of Cell Physiology & Pharmacology, University of Leicester, Leicester, UK and [3]Department of Computing Science and Mathematics, University of Stirling, Stirling, UK

The neuronal form of nitric oxide synthase (nNOS) is widely expressed in the brain and via coupling to NMDA receptor-mediated calcium influx, it is linked to synaptic plasticity (Bon & Garthwaite, 2003). However, its physiological activation and the mechanisms by which nitric oxide (NO) acts to affect neuronal excitability have proved elusive. Here, we exploit the unique input-specificity of the calyx of Held synapse to characterise NO release at this model glutamatergic synapse in the auditory pathway in acute brain slices. CBA/CaJ mice (P10–P15) were killed by decapitation in accordance with the UK Animals (Scientific Procedures) Act 1986. Brainstem slices containing the superior olivary complex were prepared as previously described (Wong *et al*., 2003) and imaging experiments were performed at 36°C on principal neurons of the medial nucleus of the trapezoid body (MNTB). Synaptic activity was achieved by midline stimulation using a bipolar electrode. Immunohistochemistry showed that nNOS is present in the cytoplasm of principle neurons in the MNTB. Slices and/or single cells were loaded with DAR-4M AM (10μM) and FURA 2 AM (10μM) and excited at 560 and 380nm to monitor NO and $[Ca^{2+}]_i$, respectively. We show that synaptic activity at the calyx of Held causes

a NMDA receptor-dependent release of NO in postsynaptic neurons. The fluorescence ratio of two repeated stimuli (F2/F1) was 1.5±0.1 (n=13 cells) for control and was suppressed by AP-5 (50μM), DNQX (10μM) and the two NOS antagonists N-PLA (10μM) and 1400W (10μM) (0.45±0.08*; 0.88±0.06*; 0.33±0.07*; 0.77±0.09* and 0.46±0.1*, respectively, n=3-12 cells, p<0.05). Synaptic activity also increased cGMP levels (basal: from 4.87±0.84 pmol mg^{-1} protein to: 21.86±3.67* pmol mg^{-1} protein, n=7-9 slices, p<0.05) which required action potential propagation and nNOS activity. Release of NO from active neurons also raised NO-dependent DAR-4M fluorescence in adjacent non-active neurons indicating the volume diffusion of NO. This diffusion between neurons was suppressed by the NO scavenger PTIO (100μM). This data supports the hypothesis that NO serves as a volume transmitter at the calyx of Held/MNTB, integrating spontaneous and evoked neuronal firing to provide an index of global activity, thereby regulating excitability and/or synaptic strength across a population of neurons and providing a significant homeostatic control of physiological functions.
Results are reported as mean±SEM. The comparison of different groups was carried out using two-tailed Student's t-test. One way ANOVA was applied for testing statistical significance between more then 2 data sets. Differences were considered statistically significant at p<0.05.

Bon CL & Garthwaite J. (2003). J Neurosci **23**, 1941-1948.

Wong AY *et al*. (2003). J Neurosci **23**, 4868-4877.

This work was funded by the MRC.

Authors have confirmed where relevant, that experiments on animals and man were conducted in accordance with national and/or local ethical requirements.

C6

Nitric oxide–dependent modulation of postsynaptic excitability in the mouse auditory brainstem

I.D. Forsythe[1], C. Kopp-Scheinpflug[2], C. Baker[1], S.J. Griffin[1], B.P. Graham[3] and J.R. Steinert[1]

[1]MRC Toxicology Unit, Leicester, UK, [2]Institute of Biology II, University of Leipzig, Leipzig, Germany and [3]Department of Computing Science and Mathematics, University of Stirling, Stirling, UK

Voltage-gated potassium (Kv) channels are widely expressed in the central nervous system and serve to regulate neuronal excitability. High voltage-activated K^+ channels are responsible for shaping action potential (AP) waveforms, thereby enhancing high frequency transmission (Rudy & McBain, 2001). Here, we exploit the calyx of Held synapse to characterize the effects of nitric oxide (NO) on K^+ channels at this glutamatergic synapse *in vitro*. CBA/CaJ mice (P10–P15) were killed by decapitation in accordance with the UK Animals (Scientific Procedures) Act 1986. Brainstem slices were prepared as previously described (Wong *et al*., 2003) and patch clamp experiments were performed at 36°C on principal neurons of the medial nucleus of the trapezoid body (MNTB). Synaptic responses were achieved by midline stimulation using a bipolar electrode, inducing activity-dependent release of NO which suppressed high voltage-activated K^+ currents over a time period of 10-20 min (control: 13.1±1.0 nA vs synaptic stimulation: 7.0±1.3* nA, n=5, p<0.05, paired t-test). Comparable suppression was achieved by perfusion of two different NO donors (control: 16.9±0.3 nA, 100μM SNP: 6.9±1.0* nA, 100μM DEANONOate: 5.4±1.5* nA, n=58-5, p<0.05). This reduction in current was prevented by incubation with antagonists of soluble guanylate cyclase and PKG (1μM ODQ: control: 14.3±2.2 nA vs SNP: 13.5±2.4 nA and 1μM KT5823: control: 19.7±0.3 nA vs SNP: 19.0±0.9 nA). Inhibition of postsynaptic Kv3 currents by TEA (3 mM), NO donors (SNP, DEANONOate, both 100μM) or synaptic activity each independently increased AP half-widths which was also modeled by a 60% reduction in the Kv3-mediated current with a single compartment model of a MNTB neuron (constructed using NEURON simulation software). Similar changes in AP waveforms were observed from *in vivo* recordings following sound exposure. NO signaling modulated the ability of neurons to faithfully follow high frequency transmission causing failures at frequencies higher then 50Hz and converting transmission from a phasic to an onset pattern. In trains of APs with Poisson-distributed inter-spike-intervals, the mean MNTB firing rate dropped from 82.1±5.5Hz to 38.5±7.9* Hz (n=4, p<0.05, paired t-test). In addition to the NO actions in synaptically targeted neurons, NO suppressed Kv3 currents by diffusion to adjacent inactive neurons (control: 12.9±1.1 nA vs synaptic stimulation: 8.8±0.9* nA, n=5, p<0.05, paired t-test) thereby modulating excitability in a diffusion-limited volume (see Abstract by Steinert *et al*. at this meeting). We conclude that NO is an endogenous modulator of postsynaptic excitability and information transmission in the auditory brainstem.
Results are reported as mean±SEM. Comparisons were carried out using two-tailed Student's t-test. Differences were considered statistically significant at p<0.05.

Rudy B & McBain CJ. (2001). *Trends Neurosci* **24**, 517-526

Wong AY *et al*. (2003). *J Neurosci* **23**, 4868-4877.

Steinert JR *et al*. (2008) presented at this meeting

This work was funded by the MRC.

Authors have confirmed where relevant, that experiments on animals and man were conducted in accordance with national and/or local ethical requirements.

C7

Generation of functional GABA neurons from mouse embryonic stem cells

E. Shin, M.J. Palmer and R.A. Fricker-Gates

Institute for science and technology in medicine, Keele University, Newcastle-under-lyme, Staffordshire, UK

Huntington's disease (HD) is a neurodegenerative disease, which is caused by expression of the mutant protein huntingtin, resulting in selective neuronal cell death in the striatum and cortex. Cell replacement using foetal tissues has been tried

showing some success in animal models and HD patients. However, the use of aborted foetal tissues raises ethical issues, and has hindered the procedure technically, requiring researchers to look for substitute cells. Because of their pluripotency and indefinite cell division, embryonic stem (ES) cells are very good candidate. We have been trying to differentiate mouse ES cells to functional striatal GABA neurons efficiently in order to transplant cells to a mouse HD model. Three different differentiation protocols – monolayer method, embryoid body method, and five stage method – have been used and all of them yielded similar percentage of GABA neurons from ES cells, based on immunocytochemical expression of appropriate markers. GABA neurons derived from ES cells using monolayer method were tested for their function compared to primary lateral ganglionic eminence (LGE) neurons, using patch clamp techniques. Primary and ES-derived neurons had inward sodium and outward potassium currents, fired sodium channel-dependent action potentials (APs), and showed spontaneous AP firing and APs after hyperpolarisation. Both LGE neurons and ES cell-derived neurons had comparable resting membrane potentials, AP thresholds, AP amplitudes, and input resistances; but significantly different current thresholds for AP firing, AP durations, and membrane capacitances. Both types of neurons responded to L-glutamate, AMPA, and aspartate, proving the existence of functional glutamate receptors. Therefore ES-derived cells not only look like neurons but also function similarly to striatal neurons derived from the LGE.

Electrophysiological properties of primary lateral ganglionic eminence neurons and mouse embryonic stem cell-derived neurons

	Primary	ES
Input resistance (MΩ) n=10	1782±303	2011±394
Resting membrane potential (mV) n=31	-77±3	-71±2
Action potential threshold (mV) n=7	-42±1	-41±2
Action potential amplitude (mV) n=7	57±3	54±2
Current threshold (pA) n=10	23±4	2±2***
Action potential duration (ms) n=7	4±0	7±1**
Membrane capacitance (pF) n=10	15±1	10±1*

*P<0.05, **P<0.01, ***P<0.001

Dunnett SB, Rosser AE (2004) NeuroRx 1:394-405

Martin GR (1981) Proc Natl Acad Sci USA 78:7634-7638

Ying QL et al. (2003) Nat Biotechnol 21:183-186

Bain G et al. (1995) Dev Biol 168:342-357

Okabe S et al. (1996) Mech Dev 59:89-102

Dr Rosemary A Fricker-Gates is my lead supervisor.

Dr Mary J Palmer has trained and let me use the patch clamping machine and advised.

Dr Meng Li in Imperial College London provided us with the 46C mouse ES cells.

Keele medical school funded this project.

Authors have confirmed where relevant, that experiments on animals and man were conducted in accordance with national and/or local ethical requirements.

C8

Repeated restraint stress enhances expression of Bcl-2, mTOR and proteasome in hippocampus

M.A. Orlovsky, Y.V. Lebed, V.E. Dosenko and G.G. Skibo

Bogomoletz Institute of Physiology, Kyiv, Ukraine

Background: Chronic stress is known to induce hippocampal neuronal loss which can lead to depression disorders in humans (1). Stress-induced hippocampal damage is believed to be related to the neurotoxic activity of glucocorticoid hormones (2), however the intracellular mechanisms of this action are still obscure. We had studied the effects of repeated restraint stress on the mRNA expression of factors, related to the neuronal survival and viability: Bcl-2 (anti-apoptotic factor), mamallian target of rapamycin (mTOR) and proteasome subunits β5 and β9 (PSM). mTOR stimulates mRNA translation through phosphorylation of some translation factors (4E-BP1, p70S6K, rpS6) thus coordinating cell growth and neuroplasticity (3).
Methods: Male Wistar rats (230-250 gr) underwent 4 hour of restraint stress in plastic tubes once per day for 10 days. Bcl-2, mTOR, PSM5β and PSM9β mRNA expression were studied in left-side hippocampus at the end of the experiments using real-time RT-PCR technique. Right hippocampus of each animal were immunohistochemically studied and the amount of NeuN-positive neuronal cells were measured in order to estimate the degree of neuronal loss. Numeric data are presented as mean±S.E.M, statistical significance as false-positive probabilities (p) computed using Student's t-test and Student's distribution.
Results: Chronic restraint led to a significant body mass loss (-5.9% compared to +4.0% gain in control group), 1.5-fold increase in adrenal gland weight and thymic atrophy. Restraint also resulted in significant neuronal loss in hippocampus: amount of NeuN-positive cells were reduced from 195.4±4.0 cells per mm (N=35) to 172.1±3.1 cells per mm (N=21) in CA1 area; from 198.7±10.5 (N=16) to 141.6±6.9 (N=22) cells per mm in CA2 and from 156.2±5.4 (N=31) to 104.9±17.7 (N=16) cells per mm in CA3. Average Bcl-2 mRNA levels in hippocampus of chronically stressed rats were significantly elevated from 5.97±0.29 (N=11) to 8.88±0.29 (N=11) c.u. ($p < 0.001$). This was accompanied by the increase in mTOR mRNA levels from 3.15±0.23 (N=8) to 3.85±0.13 (N=8) c.u. ($p < 0.05$) what goes in line with the data obtained by (3), who observed increase in mTOR activity in response to a traumatic stress. PSMβ5 mRNA levels did not undergo significant changes while PSMβ9 expression was 1.5-times enhanced from 4.81±0.39 (N=8) to 7.47±1.03 (N=8) c.u. ($p < 0.05$).
Conslusion: Together, these results suggest that changes in bcl2 pathways, mRNA translation and protein degradation may be the mechanisms contributing to the neuronal loss caused by chronic restraint stress.

Alfonso J et al. (2004). Eur J Neurosci 19, 659-666.

Höschl C & Hajek T (2001). Clin Neurosci 251 Suppl 2, 81-88.

Chen S et al. (2007). J Cereb Blood Flow Metab, 27, 939-949.

This investigation was supported, in part, by the Ukrainian State Foundation for the Fundamental Investigations grant given to Dr Orlovsky MA.

Authors have confirmed where relevant, that experiments on animals and man were conducted in accordance with national and/or local ethical requirements.

C9

Cerebral exchange kinetics of nitrite and calcitonin gene-related peptide in acute mountain sickness

D.M. Bailey[1], S. Taudorf[2], R.M. Berg[2], C. Lundby[3], K.A. Evans[1], L.T. Jensen[4], P.E. James[5], B.K. Pedersen[2] and K. Möller[2,6]

[1]Faculty of Health, Science and Sport, University of Glamorgan, South Wales, UK, [2]Department of Infectious Diseases, University of Copenhagen, Copenhagen, Denmark, [3]Copenhagen Muscle Research Centre, University of Copenhagen, Copenhagen, Denmark, [4]Institute of Experimental Research, University of Copenhagen, Copenhagen, Denmark, [5]Wales Heart Research Institute, School of Medicine Cardiff University, Cardiff, UK and [6]Department of Cardiothoracic Anaesthesia and Intensive Care Unit 4131, University of Copenhagen, Copenhagen, Denmark

An increased formation of nitric oxide (NO) and calcitonin gene-related peptide (CGRP) by the human brain in hypoxia may be implicated in the pathophysiology of acute mountain sickness (AMS) through direct activation of the trigemino-vascular system.

To test this hypothesis, we examined eleven healthy males aged 27 (mean) ± 4 (SD) years in normoxia (21.0%O_2) and following 9h passive exposure to normobaric hypoxia (12.9%O_2). Symptoms of AMS were recorded using the Lake Louise (LL) and Environmental Symptoms Questionnaire-Cerebral Symptoms (ESQ-C) scoring systems and headache determined using a visual analogue scale. Blood samples were obtained simultaneously from the radial artery and right internal jugular vein and assayed for plasma nitrite (NO_2^-) using ozone chemiluminescence and CGRP via radio-immunoassay. Global cerebral blood flow (CBF) was determined in the desaturation mode using inhaled nitrous oxide (5%) as the tracer (Kety and Schmidt, 1945). Cerebral plasma flow (CPF) was calculated as CBF x (1-haematocrit) and net flux determined as CPF x arterio-venous concentration difference ($a\text{-}v_{diff}$).

Hypoxia increased the LL (3.0 ± 1.9 *vs.* 0 ± 0 points, $P < 0.05$ *vs.* normoxia), ESQ-C (0.730 ± 0.683 *vs.* 0.000 ± 0.000 points, $P < 0.05$), and headache (20 ± 18 *vs.* 0 ± 0 mm, $P < 0.05$) scores (paired samples *t*-tests). CBF changed from 85 ± 15 to 96 ± 17 mL/100g/min in hypoxia ($P = 0.09$). Normoxia was associated with a positive $a\text{-}v_{diff}$ for NO_2^- (consistent with an influx) that was blunted by hypoxia due primarily to a reduction in arterial inflow (Table 1). In contrast, hypoxia affected neither arterial CGRP nor cerebral exchange and no relationships were observed between the change (hypoxia-normoxia) in the net flux of NO_2^- or CGRP respectively and LL (r = -0.14/-0.10), ESQ-C (r = -0.35/-0.23) or VAS (r = 0.33/-0.11) scores ($P > 0.05$, Pearson Product Moment Correlation).

In conclusion, our findings do not support a role for increased cerebral formation of NO_2^- and CGRP as molecular risk factors for AMS. On the contrary, hypoxia blunted the cerebral uptake of NO_2^-. Whether this reflects decreased consumption subsequent to a free radical-mediated reduction in systemic NO bioavailability and/or PO_2-driven re-apportionment of NO is the focus of current attention.

Table 1. Cerebral exchange

Inspirate:	Normoxia		Hypoxia	
Sample site:	Arterial	Venous	Arterial	Venous
NO_2^- (nmol/L)	474 ± 199	234 ± 85	291 ± 119*	277 ± 105
	Hypoxia < Normoxia (P < 0.05); Venous < Arterial (P < 0.05)			
Net flux (nmol/min/g)	124 ± 90		11 ± 47*	
CGRP (pmol/L)	71 ± 17	70 ± 16	70 ± 20	68 ± 20
Net flux (pmol/min/g)	0 ± 1		1 ± 2	

Values are mean ± SD; two-way repeated measures analysis of variance with paired samples *t*-tests; * different vs. normoxia ($P < 0.05$).

Kety SS and Schmidt CF (1945). *Am J Physiol* **143**, 53-66.

Authors have confirmed where relevant, that experiments on animals and man were conducted in accordance with national and/or local ethical requirements.

C10

Acute mountain sickness does not alter the coagulation cascade differently in susceptible and non-susceptible individuals

L. Fall[1], K.A. Evans[1], P.N. Ainsle[2], P. Martins[1], E. Kewley[1] and D.M. Bailey[1]

[1]Department of Science and Sport, University Of Glamorgan, Pontypridd, Wales, UK and [2]Department of Physiology, University of Otago, Otago, New Zealand

Introduction: Previous research in our laboratory has identified that the neurological components of AMS, especially headache are a potential consequence of oxidative stress. Since activation of the coagulation cascade is potentially subject to redox regulation in-vivo, the current study aimed to assess the haemostatic differences in AMS (+) and AMS (-) individuals.

Methods: Following local ethical approval, and after gaining written, informed consent, 18 apparently healthy male volunteers were recruited.

Subjects were assigned days to attend the laboratory to be administered 6 hours passive exposure to normobaric hypoxia (Fraction of inspired oxygen [F_IO_2] 12%) in an environmental chamber. After 6 hours exposure, the subjects were asked to perform an incremental cycling test to volitional exhaustion. Blood was sampled at four time points F_IO_2 21% [Normoxia], 6 hours passive hypoxic exposure [Hypoxia (rest)], immediately post exercise in hypoxia [Hypoxia (Exercise)] and at 8 hours exposure: [Hypoxia (Recovery)].

Blood was sampled via an in-dwelling cannula into sodium citrate vaccutainers and tested for plasma levels of Fibrinogen (FB), Prothrombin Time (PT), Thrombin Time (TT) and Activated Thromboplastine Time (aPTT) using a Futura Pluss Coagulometer.

AMS was diagnosed using the Lake Louise (LL) score (clinical + self-assessment scores) of ≥5 points and an Environmental Symptoms Questionnaires (ESQ) cerebral score of ≥0.7 points at Hypoxia (Rest).

Wilczynski et al.(2008) J. Cell Biol., 180: 1021-1035.

Authors have confirmed where relevant, that experiments on animals and man were conducted in accordance with national and/or local ethical requirements.

C117

Spontaneous and light-driven calcium signals in the synaptic terminals of retinal bipolar cells in larval zebrafish

M.M. Dorostkar, K. Burau, E. Dreosti, B. Odermatt and L. Lagnado

Neurobiology, MRC Laboratory of Molecular Biology, Cambridge, UK

Spontaneous electrical activity in the early visual system is thought to regulate a number of processes that lead to the establishment of appropriate synaptic connections during development (Wong, 1999). This activity has been studied in detail in retinal ganglion cells, and is modulated as the retinal circuitry matures and ON and OFF bipolar cells establish connections with specific ganglion cells in the inner plexiform layer (IPL). The mechanisms that lead to spontaneous activity in retinal ganglion cells are still unclear. Furthermore, it is not known how far spontaneous activity in ganglion cells might be driven by glutamatergic synaptic inputs from bipolar cells.

We have monitored synaptic activity of bipolar cells in the retina of live zebrafish (anaesthetised by immersion in 0.016% MS222) between 3 and 9 days post fertilization (dpf) using SyGCaMP2, a genetically encoded reporter of presynaptic calcium signals (see abstract by Dreosti et al.). Spontaneous activity was detected as early as 3 dpf and two different patterns were observed: slow calcium waves with a period of 30 – 120 s, and fast regenerative calcium "spikes" which rose in 0.5 – 0.8 s and decayed exponentially with a time-constant of 1.5 – 4.5 s. A given terminal displayed either fast spikes or slow waves in calcium, but not both. The frequency and pattern of calcium spikes varied widely between terminals, and occured at instantaneous frequencies up to 1 Hz. The percentage of terminals generating calcium spikes reached 77% (n=39) at 5 dpf, declining to 30% at 9 dpf (n=23). In contrast, slow calcium signals were most prevalent at 3 dpf (46 %; n=35), declining to 4% (n=23) at 9 dpf.

In some terminals, uniform steps of light lasting 30 s caused either a steady increase or decrease in presynaptic calcium, identifying ON and OFF cells. The percentage of terminals displaying responses to light increased from about 6% at 3 dpf (n=35) to 65% at 9 dpf (n=23). About 8% of the terminals responsive to light (n=48) generated spontaneous calcium spikes, and none exhibited slow waves. Thus the development of responsivity to light was correlated with a decrease in spontaneous synaptic activity. These results suggest that synaptic transmission from bipolar cells is one of the mechanisms generating spontaneous spikes in ganglion cells over the period that the retinal circuit is developing.

Wong ROL (1999). Retinal waves and visual system development. Annual Review of Neuroscience 22(1), 29–47.

Funded by the Medical Research Council, the Wellcome Trust and the Austrian Science Fund (FWF).

Authors have confirmed where relevant, that experiments on animals and man were conducted in accordance with national and/or local ethical requirements.

PC1

Blocking glial intercellular communication impedes axonal conduction in the isolated rat optic nerve

P.S. Hurst, K. Sakha and A.M. Butt

School of Pharmacy and Biomedical Sciences, University of Portsmouth, Portsmouth, UK

Astrocytes communicate with each other by the release of the 'gliotransmitter' ATP. It is hypothesized that intercellular communication between astrocytes may help to synchronise their activity. A primary function of astrocytes is the regulation of extracellular potassium ($[K^+]_o$), by the process of potassium spatial buffering. In the absence of effective $[K^+]_o$ regulation, the build-up of K^+ released during axonal activity results in a conduction block. Here, we have examined the effects of blocking gap junctions (GJ) and ATP-mediated communication between astrocytes on axonal excitability, in the isolated intact rat optic nerve.

Rats of the Wistar strain, aged postnatal day (P)15-20 were killed humanely by cervical dislocation, in accordance with Home Office regulations. Optic nerves were isolated intact and removed to a brain slice chamber where they were continuously perfused with artificial cerebrospinal fluid (aCSF). The compound action potential (CAP) was measured using suction electrodes, during stimulation at 1 Hz, to serve as a baseline, and during increased stimulation at 20Hz or 35Hz for 120s. The effects of the following were examined, all at 100μM (added directly to aCSF): $BaCl_2$ to block glial Kir; carbenoxolone to block GJ; and the non-specific P2 receptor antagonist suramin, and the P2X7 receptor antagonist oxidized ATP (oATP), to block ATP-mediated intercellular communication. Results were tested for significance using one way-ANOVA with post-hoc Newman-Keuls test (significance was set at $p<0.05$ for all statistical analysis, n=4-6 for all observations). In aCSF, stimulation at 20Hz or 35 Hz for 120s resulted in a significant and activity-dependent decay in the CAP (Table 1). This decay was significantly greater following treatment with $BaCl_2$, oATP or suramin, but not carbenoxolone. In the case of suramin and oATP, the effects were greater at 35Hz than 20Hz.

The results indicate that blocking Kir caused a significant decay in optic nerve conduction, and that blocking P2 and P2X7 receptors had an equivalent effect. This study supports a role for ATP-mediated astrocyte communication in $[K^+]_o$ regulation and maintaining axonal action potential conduction.

Table 1. CAP amplitude during stimulation at 20 Hz or 35Hz

	20Hz	35Hz
aCSF	67 ± 8.7%*†	46 ± 6.9%* †
BaCl2	22 ± 1.1%*	-
Carbenoxolone	45 ± 4.4%*	-
Suramin	51 ± 6.9*†	26 ± 3.7* †‡
oATP	38 ± 5.5%* †‡	13 ± 3.5* †‡

Results are mean ± SEM % CAP at 120s compared to basline CAP at 0s. *significant difference from CAP at 0s. significant difference between 20 and 35Hz. significant difference between aCSF and treated.

Supported by the BBSRC

Authors have confirmed where relevant, that experiments on animals and man were conducted in accordance with national and/or local ethical requirements.

PC2

Photoreceptor light adaptation is modulated by monopolar cell feedback in *D. melanogaster*

P. Gonzalez-Bellido, T.J. Wardill and M. Juusola

Biomedical Science, University of Sheffield, Sheffield, South Yorkshire, UK

Light adaptation in photoreceptor cells is a prerequisite for normal vision in the vastly variable light intensities found in natural environments. We investigated *in vivo* how the feedback from large monopolar cells (LMCs) onto photoreceptors modulates this process by recording intracellular voltage responses of photoreceptors in the mutants *Vam* and *ort*^{5}. In *Vam* flies, LMCs 1 and 2 degenerate and *ort*^{5} flies are a null mutant for the histamine receptor in LMCs.

By repeating saturating light pulses of 4 LEDs, we show that both *Vam* and *ort*^{5} have faster response dynamics (A, inset). From trace 2 onwards, *Vam* responses are significantly smaller than wild type (Canton S) while *ort*^{5} showed no difference to wild type (A, Trace 2, p = 0.00036 & p = 0.65 respectively, t-test), leaving *Vam* with a smaller voltage range for extra light adaptation. All flies showed a further reduction in amplitude recorded in response to 100 LEDs, highlighting a general lateral inhibitory field effect (B) which was proportionally larger in *Vam* photoreceptors (C). Both mutants displayed slower repolarisation in response to a long light pulse (D & E, arrows). *Vam* also lacked a sustained response during the first light pulse (D, asterisk), a phenotype not previously reported in mutants with defective or absent LMCs.

Our results provide further evidence that the LMC feedback actively modulates photoreceptor voltage responses[1]. Without such feedback, the photoreceptors light adaptation is defective, resulting in suboptimal use of response range for coding of visual information. Future work includes ablation of LMCs with ricin using the UAS-Gal4 system. This approach will clarify whether the missing sustained response during the first prolonged light pulse in *Vam* is solely attributable to a lack of LMCs 1 and 2.

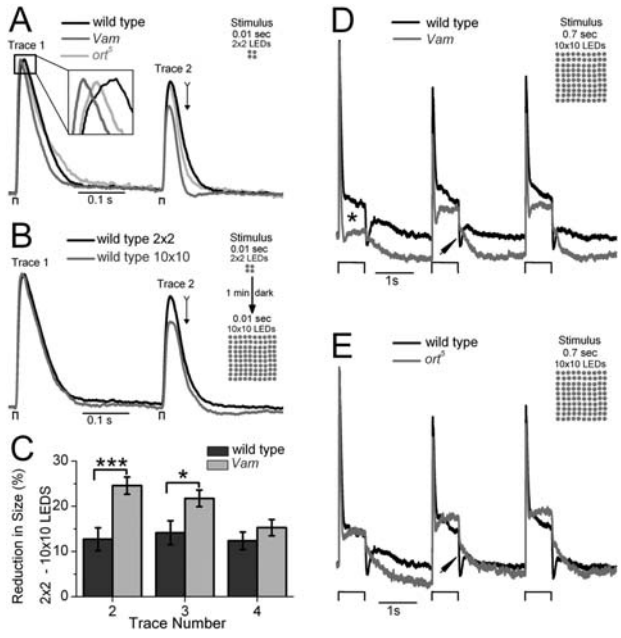

Figure 1. **A.** Mean of normalised voltage responses from wild type (n = 20, black), *Vam* (n = 14, dark grey) and *ort*^{5} (n = 6, light grey) to stimuli of 0.01 s with 4 white LEDs. **B.** The thin black arrow indicates differences between the means of normalised wild type responses to 4 (black) and 100 (grey) LEDs, with 1 min of darkness between stimuli matrices. **C.** Bar graphs compare the reduction in normalised responses to trace 1 in wild type and *Vam* when using 100 instead of 4 LEDs (***p = 0.001 & *p = 0.02669 for traces 2 and 3 respectively, t-test, error bars = S.E.). Mean of normalized responses to 0.7 s 100 LED stimuli for **D.** wild type and *Vam* and **E.** wild type and *ort*^{5}.

Zheng *et al.* (2006). *J Gen Physiol* **127**, 495–510.

This research is funded by the University of Sheffield, the BBSRC, the Royal Society and the Gatsby Foundation.

Authors have confirmed where relevant, that experiments on animals and man were conducted in accordance with national and/or local ethical requirements.

PC3

How does the *Drosophila* brain compute and see visual motion?

T.J. Wardill and M. Juusola

Department of Biomedical Science, University of Sheffield, Sheffield, UK

We wish to study how visual motion-sensitive information is routed to and processed in *Drosophila* lobula plate tangential neurones (LPTNs) for understanding visual behaviour. Compared to higher organisms, the relatively simple and genetically malleable connections between *Drosophila* LPTNs, the eyes and brain can help us to make sense of motion coding strategies. Using transgenic flies which we have developed to be predominantly UV-sensitive while selectively expressing Ca^{2+}-reporters (Cameleon) in their LPTNs ("UV-flies", Figure 1), we have been able to record intracellular voltage and Ca^{2+} signals

in LPTNs in response to moving light patterns *in vivo*. By genetically shifting the sensitivity of R1-R6 photoreceptors to UV-range, the visual excitation of photoreceptors does not overlap with the fluorescent genetic reporter, enabling us to undertake real-time Ca^{2+} imaging without influencing visual functions.

Building on these efforts, we wish to now dissect the bottom-up and top-down connections to LPTNs, and their respective roles in computing neural representations of motion signals. This we plan to do by recording changes in voltage and Ca^{2+} signals of LPTNs to moving UV-stimuli while switching on/off different synaptic inputs to them. This can be achieved by using the UAS-Gal4 system to express light gated channels, NpHR to inhibit or ChR2 to excite neurons, or express temperature sensitive endocytosis blocking proteins, such as shibire^{ts1}. To undertake this task, we are constructing a hybrid instrument that combines 2-photon scanning microscopy and electrophysiology, capable of simultaneous measurements of voltage and Ca^{2+} signals in the tissue depths and spatial resolution that are required here. Furthermore, to correlate the changes in the network activity to the fly's optomotor behaviour, our UV transgenic flies will be tested in a UV flight simulator system. The results and analysis of these experiments will be utilized for realistic mathematical modelling of motion detection.

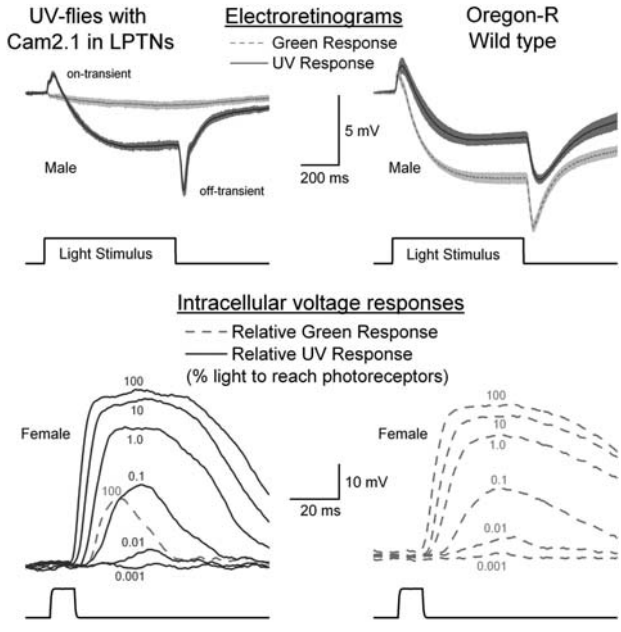

Figure 1. Responses of 'UV flies' (left) and wild type (right) to light pulses. The transients shown on electroretinograms (ERG) reflect synaptic transmission to large monopolar neurons (grey shading indicates S.E.). Wild type flies respond to both green and UV light due to the activation spectrum of Rhodopsin 1. 'UV-flies' expressing Rh4 in the place of Rh1 in photoreceptors R1-R6 show the greatest R1-R6 intracellular response to UV light with only small responses to very bright green pulses (light grey dashed traces). 'UV-flies' are >2,000 times more sensitive to UV than to green light (Wardill & Juusola, unpub.).

We thank Charles Zuker (P{ry^{+}, Rh^{1+4}}), William Pak (ry^{506}, ninaE^{17}, e^{s}) and Martin Heisenberg (P{w^{+}, Gal4-3A}) for *Drosophila* stocks. This research was supported by grants from the Biotechnology and Biological Sciences Research Council, the Gatsby Charitable Foundation and the Royal Society.

Authors have confirmed where relevant, that experiments on animals and man were conducted in accordance with national and/or local ethical requirements.

PC4

A novel negative feedback mechanism is mediated by α7 neuronal nicotinic ACh receptors in mammalian neuromuscular junction

V. Fedorin and O. Balezina

Human and Animal Physiology, Moscow State University, Moscow, Russian Federation

Neuromuscular junction endplate potentials (EPPs) decrease quickly and to a large extent during continuous stimulation. The present study examined the hypothesis that this may occur partially due to a negative feedback loop, activated by presynaptic α7 neuronal nicotinic ACh-receptors (α7-NAChR).

We stimulated a nerve in a neuromuscular preparation of isolated mouse hemidiaphragm, cut to remove the contractile response, to produce long trains of evoked EPPs at 50 Hz for prolonged periods of time (40-60 seconds). All values are presented as means with standard error of mean; statistical testing was performed using Student's paired t-test.

Substantial rundown of EPP amplitude and quantal content (measured directly as the ratio between evoked EPP and miniature EPP amplitudes) was found in the course of nerve stimulation: after 40 seconds of stimulation the quantal content of EEP was decreased to 55.2±3.1% from the initial level (n=8). This decrease was significantly attenuated by the pre-application of either α-cobratoxin (5 nM) or methyllicaconitine (100 nM) (74.2±7.2% and 76.2±7.9% respectively; n=8, $p<0.05$ in both cases), known as selective α7-NAChR antagonists. Neither antagonist changed the amplitude of miniature EPPs when applied on their own, leading us to believe that they possess no postsynaptic action.

Externally applied choline, a selective α7-NAChR agonist, decreased the quantal content of single EPPs (by 20%) and EPPs in short (1-2 sec) 50 Hz bursts of EPPs (71.6±6.1% of initial EPP after a period of 1 second stimulation *vs.* 88.6±2.1% in control; n=11, $p<0.05$). This choline-induced rundown of EPPs in a short train was similar to that caused by prolonged stimulation without exogenous choline. The depressory effect of choline was also clearly removed by concomitant application of α-cobratoxin (94.7±3.2% from initial EPP after 1 second; n=5), bringing the EPP amplitude and quantal content back to control levels.

The data obtained allows to suggest that endogenous choline, produced in the synaptic cleft by acetylcholine esterase from ACh during periods of prolonged synaptic activity, binds to a previously uncharacterized pool of pre- or perisynaptic α7-NAChR, which can down-regulate the mediator secretion in the neuromuscular junction, via a negative feedback loop. This feedback doesn't normally result in transmission failure due to a very high safety ratio of the neuromuscular synapse and is probably aimed to conserve mediator reserves over the time of prolonged rhythmic synaptic activity. Nevertheless, this negative feedback could also result in synaptic failure under certain pathological conditions that are shown to negatively affect neuromuscular transmission.

Authors have confirmed where relevant, that experiments on animals and man were conducted in accordance with national and/or local ethical requirements.

PC5

Viral short hairpin RNA knockdown of Na^+/Ca^{2+} exchanger 2 leads to enhancement of glutamatergic function and presynaptic plasticity

S.M. Mok[1], C. Glover[1], H. Scott[2], A. Bienemann[2], E. Grot[2], J. Uney[2], P. Maycox[1] and J.N. Kew[1]

[1]Psychiatry DTG, GlaxoSmithKline, Harlow, UK and [2]Henry Wellcome Laboratories for Integrated Neuroscience & Endocrinology, University of Bristol, Bristol, UK

The Na^+/Ca^{2+} exchanger (NCX) is involved in Ca^{2+} transport across the plasma membrane in excitable cells, exchanging one Ca^{2+} for three Na^+ depending on the electrochemical gradients. The NCX2 isoform is expressed in the adult brain and is thought to contribute to Ca^{2+} extrusion following neuronal excitation. Enhancing Ca^{2+}_i signalling via inhibition of NCX2 has been suggested as a possible therapeutic strategy for cognitive disorders. This study was undertaken to elucidate the contribution of NCX2 to Ca^{2+} clearance, its role in hippocampal function and the possible therapeutic window between plasticity and excitotoxicity.

A lentiviral vector expressing a short hairpin RNA targeting rat NCX2 (shNCX2) was generated, validated for NCX2 knockdown efficiency and used to transduce rat primary hippocampal neurons. Transduction of shNCX2 abolished Na^+- and Ca^{2+}-evoked responses in Fura-2 fluorescence imaging experiments, confirming ablation of NCX function. Furthermore, the Ca^{2+}_i response to glutamate application was prolonged in these neurons but was unaffected in viral-transduced controls, demonstrating the role of NCX2 in Ca^{2+} clearance following postsynaptic excitation. To investigate if NCX2 knockdown affects hippocampal function, the lentiviral vector was stereotaxically injected into the CA1 region of the hippocampus of adult Lister-Hooded rats (under isoflurane anaesthesia by inhalation). Eight weeks post-injection, *ex vivo* electrophysiological recordings of field EPSPs in the CA3-CA1 pathway were performed in hippocampal slices. An increase in the paired-pulse ratio was observed in shNCX2-transduced *vs*. EGFP-transduced slices, providing evidence for enhancement of short-term presynaptic plasticity. Increased $[Ca^{2+}]_i$ is a known trigger for excitotoxicity and we therefore tested the effect of NCX2 knockdown on cell viability using the MTT assay, a measure of mitochondrial activity. Reduced cell viability was observed in shNCX2-transduced primary hippocampal neurons the same multiplicity of infection at which enhancement of glutamate-evoked responses was observed. Taken together, these data show that inhibition of NCX2 function enhanced both pre- and postsynaptic Ca^{2+} signalling but concomitantly reduced cell viability.

Authors have confirmed where relevant, that experiments on animals and man were conducted in accordance with national and/or local ethical requirements.

PC6

Characterisation of *N*-acetyl-aspartylglutamate (NAAG) activity at mGluR2 and mGluR3

A. Fricker[1], R. De La Flor[2], S.M. Mok[1] and J.N. Kew[1]

[1]Psychiatry Discovery Technology Group, GlaxoSmithKline, New Frontier Science Park, Harlow, UK and [2]Psychiatry Centre of Excellence for Drug Discovery, GlaxoSmithKline, New Frontier Science Park, Harlow, UK

A group II metabotropic glutamate receptor (mGluR) agonist was recently reported to be clinically efficacious against positive and negative symptoms of schizophrenia (reference 1). The endogenous neuropeptide NAAG has been reported to have agonist activity at mGluR2 and mGluR3 (reference 2) and is degraded by the enzyme naaladase. Hence, elevating the concentration of NAAG by inhibition of naaladase represents a potential strategy for the treatment of schizophrenia via mGluR2/3 activation.

Presynaptic mGluR2/3 autoreceptors modulate glutamatergic neurotransmission in the hippocampus (reference 3). We investigated the effect of NAAG and the naaladase inhibitor 2PMPA on paired field EPSPs (fEPSPs) evoked by stimulation of the perforant path and recorded in the dentate gyrus mid-molecular layer in adult Sprague-Dawley rat hippocampal slices. Bath application of NAAG (100 μM; n=6) had no effect on the amplitude of the fEPSP or the paired-pulse ratio while the mGluR2/3 agonist LY379268 (1 μM; n=5) inhibited the evoked fEPSPs and increased the paired-pulse ratio (Student t test, $p<0.01$), consistent with a presynaptic inhibitory action mediated by mGluR2/3 activation.

In order to assess NAAG activity at group II mGluR more directly, we performed whole-cell voltage-clamp recordings from HEK MSRII cells transiently transfected with a human G protein-activated inwardly rectifying K^+ channel concatamer ($GIRK_{1/2}$) and either human mGluR2 or mGluR3. Glutamate-elicited inward currents were observed with EC_{50} of 18 μM and 1 μM for cells transfected with mGluR2 (n=3-5) and mGluR3 (n=3-4), respectively, and these were abolished by the mGluR2/3 antagonist LY341495 (1 μM; n=4).

NAAG was purified using a cation exchange column and purity was confirmed by HPLC coupled with fluorescence detection analysis. Application of purified NAAG (300 μM or 1 mM) onto $GIRK_{1/2}$-mGluR2 or $GIRK_{1/2}$-mGluR3 transfected cells failed to evoke responses (n=4-5), whilst subsequent glutamate application (100 μM) induced LY341495-sensitive currents.

To conclude, we found that purified NAAG had no agonist activity at group II mGluRs using the human recombinant mGluR2/3-$GIRK_{1/2}$ assay, consistent with our observations in rat hippocampal slices where NAAG and the naaladase inhibitor 2PMPA had no effect on glutamatergic transmission at the mGluR2/3-sensitive medial perforant pathway. Taken together, these findings do not support the rationale for targeting naaladase to increase brain NAAG levels as a therapeutic strategy for schizophrenia.

Patil *et al.* (2007). *Nat Med* **13**, 1102–1107

Wroblewska *et al.* (1997). *J Neurochem* **69**, 174-181

Kew *et al.* (2000). *Neuropharmacology* **40**, 20-27

Authors have confirmed where relevant, that experiments on animals and man were conducted in accordance with national and/or local ethical requirements.

PC7

Competition between memantine and magnesium for block of NMDA receptor channels in dopaminergic neurons of neonatal rat substantia nigra

Z. Huang, Y. Lo and A.J. Gibb

Neuroscience,Physiology and Pharmacology, University College London, London, UK

Activation of NMDA receptors in substantia nigra pars compacta (SNc) dopaminergic neurones induces a voltage-dependent burst firing (Johnson et al., 1992) that regulates dopamine release in the striatum. However, excessive activation of NMDA receptors generates oxidative stress and may cause excitotoxic cell death of dopamine neurones. This has been hypothesized to contribute to disease progression in PD (Blandini et al., 2000). Compared with other NMDA receptor open channel blockers, memantine is well tolerated clinically (Lipton, 2006) and has potential therapeutic utility for acute and chronic neurodegenetative diseases including stroke, acute trauma, Parkinson's disease, and Huntington's disease (Lipton, 2006). Since external Mg2+ and memantine both bind in the NMDA receptor channel, Mg2+ and memantine might compete for binding. We have used patch-clamp whole-cell recording methods to quantify the memantine block of NMDA receptors in the absence of and in the presence of physiological concentrations of external Mg2+ in 300 μm thick brain slices from 7 day old rats.
Responses to high concentration (0.1 mM) or low concentration (0.02 mM) NMDA and 0.01 mM glycine in the presence of TTX (100 nM) with 3mM ATP and 1mM GTP in the pipette solution were recorded and the voltage-dependence of the net whole-cell NMDA current evoked during voltage ramps (-100 mV to +40 mV of 2 seconds duration) in the presence of 5 μM or 50 μM memantine and in the absence or in the present of 1 mM Mg2+ were quantified using simple and trapping channel block models. Memantine inhibits NMDA receptors with higher potency (IC50 = 6 μM) when the agonist concentration is higher (0.1 mM NMDA) and has less potency (IC50 = 15 μM) at low concentrations of agonist (0.02 mM NMDA). In the absence of external Mg2+, memantine showed less voltage-dependence (δ=0.55-0.6) than Mg2+ (δ=0.82) suggesting a shallower binding site within the channel. Interestingly, as previously described by Sobolevsky et al. (1998) in hippocampal neurons, the total block was reduced during co-application of memantine (50 μM) with 1 mM external Mg2+, compared to with 1 mM Mg2+ alone (n = 8). These results are not consistent with simple competition between memantine and external Mg2+ for access to a channel binding site but can be described by models (Sobolevsky & Koshelev, 1998) that have two binding sites in the channel.

Johnson SW et al. (1992). Science 258, 665-667.

Blandini F et al. (2000). Prog Neurobiol 62, 63-68.

Lipton SA (2006). Nat Rev Drug Discov 5(2), 160-170.

Sobolevsky AI et al. (1998). J Physiol 512, 47-60.

Sobolevsky AI & Koshelev S (1998). Biophys J 74, 1305–1319.

Supported by the BBSRC. Z.H. was funded by an Overseas Research Studentship and a UCL Graduate School Old Student's Association Scholarship. Y.N.L is funded by a Scholarship from His Majesty's Government of Brunei, Darussalam.

Authors have confirmed where relevant, that experiments on animals and man were conducted in accordance with national and/or local ethical requirements.

PC8

Calcium fluxes and regulation of intracellular [Ca^{2+}] in rat intracardiac ganglion neurons: *in vitro*

J. Dyavanapalli and A.A. Harper

College of Life Sciences, University of Dundee, Dundee, UK

Ca^{2+} is a key player in the regulation of many aspects of neuronal function (Berridge 1998). Changes in $[Ca^{2+}]_i$ can come from an influx of Ca^{2+} or intracellular stores. In dissociated neonatal intracardiac ganglion (ICG) neurons major sources of increases in $[Ca^{2+}]_i$ include; Ca^{2+} entry through voltage-operated Ca^{2+} channels during the action potential and nicotinic acetylcholine receptor (nAChR) channels . This increase is amplified by release of Ca^{2+} from ryanodine-sensitive Ca^{2+} stores. Activation of muscarinic ACh receptors (mAChR) also leads to Ca^{2+} release from the endoplasmic reticulum (ER) driven by a metabotropic response (Beker et al. 2003).
We have investigated the $[Ca^{2+}]_i$ transients in adult rat ICG neurons evoked by somatic action potentials (direct stimulation), synaptic transmission evoked by vagal nerve stimulation (indirect) and focal application of ACh.
An isolated, *in vitro*, right atrial ganglionic plexus preparation was used primarily associated with regulating sinoatrial node function (Sampaio et al. 2003). Intracellular recordings were made using sharp glass microelectrodes filled with Oregon Green 488 BAPTA-1 allowing simultaneous recording of electrical properties and measurement of $[Ca^{2+}]_i$. Signals resulting from $[Ca^{2+}]_i$ changes were expressed as the ratio of fluorescence changes over baseline fluorescence, $(f\text{-}f_o)/f_o$.
The increase in $[Ca^{2+}]_i$. in response to a volley of 20 action potentials (10 Hz) evoked by indirect stimulation was not significantly different from that evoked by direct stimulation (0.70± 0.37 and 0.75 ±0.33 respectively, n=4).
ACh responses were reduced by the mAChR antagonist, atropine (1μM) and nearly eliminated by co-application of atropine and the nAChR antagonist, mecamylamine (10μM) [see Fig 1]. Ryanodine (10 μM) reduced nACh responses [evoked by selective activation of nAChR with short pulses (≤ 100 ms) of Ach] to ~0.6 of control values (n=3). Removal of external Ca^{2+} blunted but did not eliminate ACh induced responses.
Together these results are in agreement with the nicotinic and muscarinic ACh receptor activated $[Ca^{2+}]_i$ responses reported for dissociated neonatal ICG neurones (Beker et al. 2003).
In contrast to focally applied ACh there was no slow synaptic potential or $[Ca^{2+}]_i$ changes following indirect stimulation. This may be due to a difference between junctional and extrajunctional ACh receptors in these neurones.

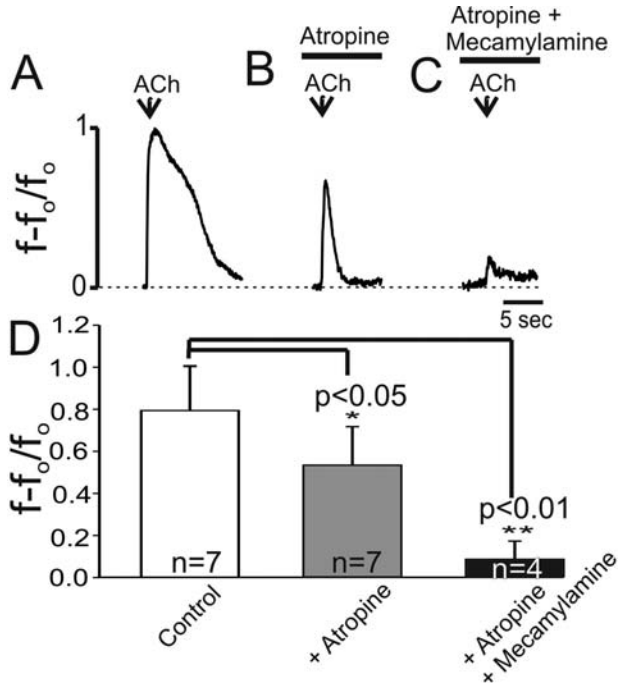

Figure 1: Representative traces of increases in $[Ca^{2+}]_i$ evoked by focally applied ACh. (100μ M, 1 s) recorded in A, control ; B, atropine; C, atropine + mecamylamine. D: bar chart of increases in $[Ca^{2+}]_i$ in response to ACh during the above maneuvers.

Berridge MJ. (1998). Neuron **21**,13-26.

Beker F *et al*. (2003). J Neurophysiol **90**, 1956-1964.

Sampaio KN *et al*. (2003). Exp Physiol **88**, 315-27.

We thank British Heart Foundation for supporting this work.

Authors have confirmed where relevant, that experiments on animals and man were conducted in accordance with national and/or local ethical requirements.

PC9

In vivo imaging of synaptic vesicle cycling in the retina of zebrafish

B. Odermatt, A. Derevier and L. Lagnado

Neurobiology, MRC-Laboratory of Molecular Biology, Cambridge, UK

Ribbon synapses of photoreceptors and bipolar cells support a continuous cycle of exocytosis and endocytosis (Lagnado et al. 1996), which is modulated by graded changes in membrane potential generated by light. The properties of this vesicle cycle have been studied in dissociated neurons, but less is known about its operation within the retina.

To investigate vesicle cycling at ribbon synapses we have made stable lines of transgenic zebrafish expressing SypHy, a genetically encoded fluorescent reporter of exocytosis and endocytosis (Granseth et al. 2006) SypHy comprises a pH-sensitive GFP fused to the second intravesicluar vesicular loop of synaptophysin, a transmembrane protein of synaptic vesicles. Using SypHy, exocytosis is reported as an increase in fluorescence and vesicle reacidification after endocytosis as a decrease. Expression of SypHy was targeted to ribbon synapses using the promoter region of ribeye, the major protein component of the ribbon. SypHy fluorescence was monitored in live zebrafish (anaesthetised by immersion in 0.016% MS222) 10-14 days post fertilisation using multiphoton microscopy, allowing the visualization of terminals through different strata of the inner plexiform layer (IPL) in the retina.

We have begun by investigating the encoding visual stimuli by the synaptic output from bipolar cells. Using spatially uniform amber light delivered from darkness and lasting for 30 s, reproducible some terminals become brighter (ON) and some dimmer (OFF). These changes reached a steady state, were reversible and the responding terminals were mainly situated in their expected strata (ON/OFF) within the IPL. The amplitude of these changes is graded with light intensity. Notably, the rate of exocytosis in ON and OFF terminals varied over a similar range and was modulated by the same light intensities. These results indicate that the intensity of steady lights are encoded symmetrically by the ON and OFF channels of the IPL.

Using SypHy, it is also possible to differentiate between the terminals of bipolar cells responding preferentially to a steady light (sustained) or flickering light (transient). This approach to identifying different functional classes of synaptic terminal within the IPL will complement the mapping of electrical and synaptic activity using reporters of the presynaptic calcium signal (Dreosti, Odermatt and Lagnado, accompanying abstract). Using these methods, we hope to build a picture of the functional organization of the IPL, as well as changes in synaptic function underlying alterations in retinal processing during different forms of adaptation.

Lagnado L et al. (1996). Neuron 17, 957-967.

Granseth B et al. (2006). Neuron 51, 773-786.

Funded by the Medical Research Council, the Wellcome Trust and the European Commission (Marie Curie fellowship to BO).

Authors have confirmed where relevant, that experiments on animals and man were conducted in accordance with national and/or local ethical requirements.

PC10

Dynamic optimization of visual information by graded synaptic signal transfer in _Drosophila_ eye

A. Nikolaev[1], L. Zheng[1], T. Wardlill[1], C.J. O'Kane[2], G.G. de Polavieja[3] and M. Juusola[1]

[1]Biomedical Sciences, University of Sheffield, Sheffield, UK, [2]Genetics, University of Cambridge, Cambridge, UK and [3]Theoretical Physics, Universidad Autónoma de Madrid, Madrid, Spain

TITLE ONLY

Authors have confirmed where relevant, that experiments on animals and man were conducted in accordance with national and/or local ethical requirements.

PC11

Bulk synaptic vesicle endocytosis is rapid and occurs only during stimulation

E. Clayton[1], G. Evans[2] and M. Cousin[1]

[1]Centre for Integrative Physiology, University of Edinburgh, Edinburgh, UK and [2]Department of Biology, University of York, York, UK

Bulk endocytosis in central nerve terminals is activated by strong stimulation, however the speed at which it is initiated and for how long it persists is still a matter of debate. To resolve this issue we performed a characterisation of bulk endocytic retrieval using a range of different stimulation paradigms. Bulk endocytosis was monitored by either the loading of the fluorescent dyes FM2-10 and FM1-43, uptake of tetramethyrhodamine-dextran (40 kDa) or morphological analysis of uptake of the fluid phase marker horse radish peroxidase. When neuronal cultures were subjected to mild stimulation (200 action potentials at 10 Hz) bulk endocytosis was not observed using any of our assay systems. However when more intense trains of action potentials (400 or 800 action potentials at 40 Hz and 80 Hz respectively) or elevated KCl were applied to neurons, bulk endocytosis was activated. Importantly bulk endocytosis ceased on termination of stimulation, whereas a single synaptic vesicle pathway persisted. Thus bulk endocytosis is a fast triggered event that occurs only during strong stimulation and provides the nerve terminal with an appropriate mechanism to meet the demands of synaptic vesicle retrieval during periods of intense synaptic vesicle exocytosis.

This work was supported by both The Wellcome Trust (Ref: GR070569) and Epilepsy Research UK. We wish to thank Dr. Alan Prescott and Mr. John James (both University of Dundee) for their excellent technical assistance.

Authors have confirmed where relevant, that experiments on animals and man were conducted in accordance with national and/or local ethical requirements.

PC12

Amyloid beta production is important for cell viability and neurite outgrowth

R. Sayer[1], T.L. Kerrigan[2], C. Peers[2] and H.A. Pearson[1]

[1]Institute of Membrane and Systems Biology, Leeds University, Leeds, UK and [2]Institue of Cardiovascular Medicine, Leeds University, Leeds, UK

Elevated levels of the amyloid beta (Aβ) peptide is one of the key pathological hallmarks of Alzheimer's disease (1). The Aβ peptide is produced by the sequential cleavage of two proteases known as β and γ secretase. $A\beta_{40}$ has previously been found at nM concentrations in the cerebrospinal fluid of healthy individuals (2) however, at present a physiological role for the Aβ peptide remains elusive. The aim of the study was to determine the effects of inhibiting the β and γ secretase enzymes initially using commercially available secretase inhibitors and subsequently by shiRNA of the BACE 1 gene to investigate a potential physiological role for the Aβ peptide.
Human SH-SY5Y neuroblastoma cells were treated with 10μM of the respective γ secretase inhibitors γI, γIV or γVI for 24 hrs, and the cell viability and caspase 3/7 activity were determined using MTT and caspase 3/7 assays respectively. Small interfering RNA (shiRNA) duplexes were designed against BACE-1. BACE 1 shiRNA was transfected into SH-SY5Y neuroblastoma cells using the GFP-tagged plentilox 3.7 virus. Reaggregate cultures of cerebellar granule neurones (CGN) were prepared and treated with either 10μM of the γ secretase inhibitors γI, γIV or γVI for 24 hrs. CGNs were fixed in 3.5 % paraformaldehyde and the neurites were immunocytochemically stained using the MAP2 neuronal marker. The neurite length from each reaggregate culture was measured using Image J software. Results are expressed as mean ± SEM. Statistical significance was assigned using One-Way ANOVA.

There was a significant reduction in cell viability and a corresponding increase in caspase 3/7 activity following treatment with γI a selective inhibitor of $A\beta_{1\text{-}40}$ (44.35 ± 3.01 % of control for cell viability) (353.4 ± 8.53 % of control for caspase 3/7), and γIV, an inhibitor of both the $A\beta_{1\text{-}40}$ and $A\beta_{42}$ peptides (54.05 ± 8.76 % of control for cell viability) (218.4±13.11 % of control for caspase 3/7). γVI, the selective $A\beta_{42}$ inhibitor had no effect on cell viability (102 ± 8.67 % of control) or caspase 3/7 activity (118.78 ± 28.04 % of control) (n=4). When the BACE 1 gene was silenced in SH-SY5Y neuroblastoma cells, this produced a decrease in cell viability (0.011± 0.001 AU/mg protein) compared to the control cells (0.020±0.002 AU/mg protein) and a corresponding increase in caspase 3/7 activity (n=4). Treatment with either 10μM γI or γIV significantly reduced neurite outgrowth in cerebellar granule reaggregate cultures (n=3). However treatment with the γVI secretase inhibitor had no effect on neurite outgrowth (n=3). The study provides evidence that the $A\beta_{1\text{-}40}$ peptide is important in neurite outgrowth and additionally in the regulation of cell survival.

Glenner GC & Wong CW (1984) *Biochem Biophys Res Commun* **120** 885-890.

Seubert P et al (1993)*Nature* **359** 325-327.

Supported by the Alzheimer's Research Trust.

Authors have confirmed where relevant, that experiments on animals and man were conducted in accordance with national and/or local ethical requirements.

PC13

Spinal cord contusion injury using a custom-made device for rat – an experimental modelling of spinal cord injury

S. Bharathy and J. Cjebaraj

AUFRG, Anna University, Chennai, Tamil nadu, India

TITLE ONLY

Authors have confirmed where relevant, that experiments on animals and man were conducted in accordance with national and/or local ethical requirements.

PC14

Lentiviral and adenoviral vectors for targeting raphe serotonergic neurones based on a transcriptional amplification strategy

K. Benzekhroufa, B. Liu, F. Tang, A.G. Teschemacher and S. Kasparov

Physiology, University of Bristol, Bristol, UK

Serotonin (5HT), one of the principal neuromodulators in the mammalian brain, is implicated in a variety of disorders such as pain, depression and schizophrenia. Many aspects of serotonergic transmission remain unknown, necessitating the development of new research tools. Previously, we successfully used viral vectors for cell-specific gene expression in the brain in order to selectively study or modulate the function of targeted neurones (Duale et al. 2007; Wang et al. 2006; Chiti & Teschemacher, 2007). Here we present novel lenti- and adenoviral vectors suitable for selective gene expression in raphe 5HT neurones. For targeting we used partial sequences (length 3.6kb, 2kb, and 1kb) of the natural promoter of rat tryptophan hydroxylase 2 (TPH2), the rate limiting enzyme in 5HT synthesis, obtained by PCR from rat brain genomic DNA. Lentiviral vectors for expression of EGFP were prepared using standard protocols (Liu et al. 2008) and stereotaxically microinjected into the rat raphe nuclei (under a mixture of ketamine (60 mg/kg) and medetomidine (250 μg/kg) i.m. anaesthesia). Specificity was then determined by immunofluorescence using anti-GFP and anti-TPH2 antibodies. The 3.6kb and 2kb promoter sequences conferred specific expression (co-localisation >95%), while the specificity of the 1kb promoter was only ~78%. However, native promoters were weak, and expression could only be detected using anti-GFP antibodies. To overcome this limitation, we employed a previously established transcriptional amplification strategy which involves cell-specific co-expression of a potent chimeric transactivator (Liu et al. 2008; Liu et al. 2006). This strategy increased the potency of 3.6kb and 2kb TPH2 promoters, leading to visible EGFP expression, while maintaining 5HT neurone specificity at 99% (n= 700 cells). Adenoviral vectors based on the 3.6kb construct were generated which caused visible EGFP expression in 5HT neurones in organotypic brainstem slice cultures. Moreover, it was possible to visually identify EGFP-positive axons with multiple small varicosities. Using previously established methods (Chiti & Teschemacher, 2007), we made the first microamperometric recordings of quantal 5HT release, and the first patch clamp recordings from EGFP-expressing 5HT neurones of the rat raphe. We believe that these viral vectors have great potential for in vivo and in vitro studies into the function of central 5HT neurones.

Chiti Z & Teschemacher AG (2007). FASEB Journal 21, 2540-2550.

Duale H, Waki H, Howorth P, Kasparov S, Teschemacher AG, & Paton JFR (2007). Cardiovascular Research 76, 184-193.

Liu BH, Wang S, Brenner M, Paton JFR, & Kasparov S (2008). Journal of Gene Medicine in press.

Liu BH, Yang Y, Paton JFR, Li F, Boulaire J, Kasparov S, & Wang S (2006). Molecular Therapy 14, 872-882.

Wang S, Teschemacher AG, Paton JF, & Kasparov S (2006). FASEB Journal 20 online, 1537-1539.

Acknowledgements: K.B. is in receipt of the Fellowship from the Ministry of Higher Education and Scientific Research of Algeria, BHL and AGT are funded by the British Heart Foundation.

Authors have confirmed where relevant, that experiments on animals and man were conducted in accordance with national and/or local ethical requirements.

PC15

The presence of mechanosensitive channels in the rainbow trout (*Oncorhynchus mykiss*) heart

S.M. Patrick[1], E. White[2] and H.A. Shiels[1]

[1]The Faculty of Life Sciences, The University of Manchester, Manchester, UK and [2]Institute of Membrane and Systems Biology, The University of Leeds, Leeds, UK

Mechanosensitivity describes the response to mechanical stimulation in cells, this may occur through the activation of mechanosensitive channels (MSCs). MSCs have been studied in microorganisms and shown to act as mechanoelectrical transducers of the forces exerted upon the cell membrane of the microorganism and so allow the cell to respond to mechanical stimuli (Martinac and Kloda, 2003). More recently, studies have found the degree of mechanosensitivity of mammalian cardiac tissue may contribute to electrical instability and arrhythmic disposition of the heart after myocardial infarction (Kamkin et al, 2005).

In this study we looked at the physiological effect of stretch upon the ventricular monophasic action potential (MAP) of the isolated whole *O.mykiss* heart (n=8). A range of filling pressures (1kPa – 4kPa) were used to stretch the heart and in some experiments outflow from the heart was inhibited to induce a large stretch of the myocardium. MAPs were recorded from the surface of the spontaneously beating heart.

An increase in filling pressure from 1kPa to 4 kPa shortened the MAP at 25% repolarisation (one way repeated measures ANOVA, P=0.017). Clamping outflow from the heart shortened this further (P=0.001). No significant differences were found in the MAP at 50% repolarisation time with either changes in filling pressure or clamping outflow. Although no significant difference in repolarisation time at 90% was seen with increased filling pressure, significant elongation (P<0.05) was seen when outflow was clamped. These experiments show that the MAP of *O. mykiss* is altered, due to stretch, in a similar manner to that which has been described in mammals (see, White, 2006) and may indicate the presence of non-selective cation MSCs in the *O.mykiss* ventricle. To investigate this further, we have cloned the trout variants of both TRPC1, which has been reported to be a store operated $Ca2^+$ MSC, and TREK-1 which has been identified as a twin pore K^+ MSC. We will use this information to look at the evolution of these channels and to determine their presence in different tissues from *O. mykiss*.